AAEC/E 106

AUSTRALIAN ATOMIC ENERGY COMMISSION

RESEARCH ESTABLISHMENT

LUCAS HEIGHTS

THE IRRADIATION BEHAVIOUR OF BERYLLIUM OXIDE DISPERSION FUELS

by

G. L. HANNA

B. S. HICKMAN

R. J. HILDITCH

Issued Sydney, March 1963

AUSTRALIAN ATOMIC ENERGY COMMISSION

RESEARCH ESTABLISHMENT

LUCAS HEIGHTS

THE IRRADIATION BEHAVIOUR OF BERYLLIUM OXIDE DISPERSION FUELS

by

G. L. HANNA

B. S. HICKMAN

R. J. HILDITCH

ABSTRACT

Specimens of beryllium oxide based dispersion fuels containing between three and twenty-six volume per cent. of $UO_2 - ThO_2$ solid solution were irradiated to fission densities of 2 to 14 x 10^{19} fissions/cm^3 of total specimen (equivalent burn-ups of 80 to 230 per cent.) at temperatures of 600 – 850 °C.

The experiment was primarily designed to investigate fission product damage although some fast neutron damage did occur in the matrix. The specimens showed excellent resistance to fission product damage; dimensional changes were small, fission product escape was generally only that expected by recoil and there was no sign of cracking due to thermal stresses although these reached estimated values of about 30,000 p.s.i. in some specimens. Metallographic examination showed that some weakening of the matrix grain boundaries had occurred and some preliminary x-ray results suggested that the matrix was in a state of strain.

It is suggested that these effects could be due either to fast neutron damage in the matrix or swelling of the fuel particles. The experiment did not provide any conclusive evidence for the superiority of coarse fuel particles (100 – 180μ) over fine fuel particles (< 10μ) although the dimensional changes and the degree of matrix strain were higher in the latter specimens.

CONTENTS

1. INTRODUCTION

As part of the Commission's research programme to evaluate the potential of beryllium oxide in a high–temperature gas–cooled (H.T.G.C.) reactor system, studies are being made of fuels in which the fissile and fertile material is dispersed throughout some or all of the moderator. The advantages of a dispersion fuel have been discussed fully by Weber (1959) and White, Beard, and Willis (1957).

From the standpoint of irradiation damage, dispersion fuels have the advantage that under certain conditions of particle size and volume of dispersed fuel, the intense fission product damage can be limited to the fuel particles, and their immediate surroundings, leaving the matrix substantially undamaged by fission fragments. However, other mechanisms can cause damage in the matrix; in the case of beryllium oxide, damage can arise from fast neutron irradiation by the production of gases from the (n, 2n) and (n, α) reactions in beryllium and by fast neutron collisions causing atomic displacements.

The fuel favoured at present for application in an H.T.G.C. reactor is a dispersion of particles of urania–thoria solid solution (U, Th)O_2 in a matrix of beryllium oxide. The irradiation–damage behaviour of this fuel has been discussed in detail by Hickman (1962a). This investigation has three main aspects:

(1) A study of the irradiation effects in beryllium oxide under fast neutron bombardment to determine the limits, in terms of irradiation dose and temperature, to which this material could be used as a moderator or fuel matrix. The status of this work has been reported recently by Hickman (1962b).

(2) A study of fission–product damage in the fuel material. Materials are irradiated in an almost pure thermal flux so that effects due to fast neutron irradiation of the matrix are small.

(3) A study of the combined effects of fast neutron and fission fragment damage by irradiating fuel specimens in neutron flux covering both fast and thermal energies.

This report presents and discusses the results of the first irradiation experiment designed to study the behaviour of the (U, Th)O_2–BeO fuel when subjected to mainly fission product damage in a thermal neutron flux.

The factors governing the choice of fuel specimen compositions were discussed by Hickman (1962a). Specimens were chosen to demonstrate the effects of specimen composition (that is, volume fraction of fuel phase), fuel particle size, burn–up, and thermal stress. The influence of each of these variables on the choice of specimens is as follows:

(i) Composition: When the experiment was initiated, the composition of an actual reactor fuel had not been defined, but preliminary surveys indicated that the heavy metal:beryllium atom ratio would be between 31:250 to 31:3000 with the uranium:thorium ratio about 1:30. For this experiment, specimens were chosen with ratios of 31:250, 31:500, 31:1000, 31:2000, and 31:3000 (that is, 25.8, 15.7, 8.4, 4.4, and 3.0 volume per cent. (U Th)O_2 respectively).

(ii) Fuel Particle Size: For most specimens the fuel particle diameter was 100 – 185 microns, a size which theoretically gives a low matrix damage due to fission fragment recoil (Hickman 1962a). The theoretical amount of matrix damage for each composition is given in Table 1. For coarse dispersions damage ranges from 3.1 to 27.5 per cent. Two specimens (numbered 148/149 and 150/153) having a fuel particle size of less than 10 microns were included to cover the case where all the matrix is damaged by fission recoil and over 99 per cent. of the fission products escape from the particles.

(iii) Burn–up: The equivalent burn–up * was planned to be approximately 100 per cent. in six sets of specimens and approximately 250 per cent. in the remaining two sets. To accelerate the damage rate some of the thorium (assuming a uranium:thorium ratio of 1:30) was replaced by U–235. Thus, three batches of fuel material were used having fissile:fertile ratios of 8:23, 16:15 and 25:6.

* Note: The term equivalent burn–up is used to relate the burn–up in the test specimens to that in the fuel mixtures of actual reactor systems.

It is defined by:

$$\text{Equivalent burn-up, \%} = \frac{N_f \times 100}{N} \quad ,$$

where N_f is the number of atoms per unit volume fissioned in the test specimen and N the number of U-235 atoms per unit volume in a fuel mixture of the same heavy metal:beryllium ratio but a U:Th ratio of 1:30.

(iv) Temperature: Specimen temperatures were designed to cover the range 600 to 700 °C.

(v) Thermal Stress: Estimated thermal stresses for the above temperatures ranged up to about 23000 p.s.i. depending on specimen diameter and composition. Note. The thermal stresses given in the original proposal (Hickman 1958) were much lower than this (11,000 p.s.i. maximum)owing to the use of incorrect data in the calculations.

As high density specimens of the desired height to diameter ratio could not be fabricated by hot pressing (the only method feasible at the time) they were prepared in two halves which were held in end-to-end contact during irradiation. Each half-specimen was allotted an individual number and throughout this report each twin specimen will be denoted by two numbers, for example 100/101 to 150/153. Eight duplicate pairs of twin specimens (that is, thirty-two half-specimens) were irradiated in order to cover the desired variables and one specimen similar to each pair was given a heat treatment without irradiation to enable thermal effects to be differentiated from irradiation effects. Details of composition and density are given in Table 1. Densities were 94-99 per cent. of theoretical.

2. EXPERIMENTAL PROCEDURE

2.1 Specimen Preparation

A detailed description of specimen preparation has been given by Reeve and Ramm (1960). The materials used were Mallinkrodt UO_2 enriched to 90V, ThO_2 calcined to 600 °C and Pechiney BeO calcined at 900 - 950 °C.

The three batches of $UO_2 - ThO_2$ solid solution $[(U,Th)O_2]$ were prepared by hot-pressing the mixed oxide powders at 1800 °C and 1 t.s.i. for 30 minutes. Crushing of these compacts gave only 30 - 35 per cent. recovery in the 100 - 185 micron range and the fines were re-cycled to increase the yield. Material of 8:23 molar ratio was compounded directly from the pure oxides but material of the other two compositions was obtained by utilising the excess fines of the 8:23 material, adding sufficient UO_2 to give the correct composition.

The dispersion specimens themselves were fabricated from carefully compounded powder mixtures of the $(U,Th)O_2$ solution and beryllium oxide by hot pressing at 1750 °C and 1 t.s.i. Compacts 4 cm diameter by 1.7 cm high were made, and from each compact seven slightly oversize specimens were produced as drill cores using a hollow diamond-impregnated drill. These were ground to final dimensions (0.0025 cm tolerance) using a tool post grinding attachment on a lathe.

One specimen in each set of seven had a ⅛ inch hole drilled centrally along its axis to provide thermocouple pockets for in-pile temperature measurement. Centre temperatures were measured in one stringer only so that most specimens would be solid cylinders.

Photographs of typical specimens are shown in Figure 4.

2.2 Pre-Irradiation Examination

The following points, relevant to the as-fabricated condition of the specimens are abstracted from Reeve and Ramm (1960).

(i) The three batches of fuel material gave sharp X-ray diffraction patterns free of reflections from the pure oxides. This implies that they were well homogenised.

(ii) Chemical analysis showed only minor variations from the prescribed compositions.

(iii) Gamma spectrometry on undrilled specimens revealed the following specimen-to-specimen variations in the weight of U-235 contained:

Specimens	100 - 104, 142 - 153,	± 3%
	106 - 110,	± 7½%
	136 - 141,	+ 1 to -3%

No variations were detected in specimens 112 - 129.

(iv) Optical measurements of fuel particles showed them to be mostly plate or needle-like in shape. The two longer dimensions of randomly chosen particles are given in Table 2. Some fine particles - thought to be the result of abrasion during mixing with BeO - were seen in metallography samples typical of specimens 100 to 135; the mean particle size in these specimens will therefore be smaller than that shown in Table 2.

(v) Fuel particles were aligned with their longer axes perpendicular to the pressing direction.

(vi) Porosity within the fuel grains themselves was variable, being negligible in some and up to about 25 per cent. (estimated) in others. The more porous particles were thought to be due to the recycling of fines which compacted less readily than the pure oxide mixtures.

(vii) The uniformity of fuel dispersion was reasonably good (see Figure 1).

(viii) A similar dispersion of fine porosity was found in the matrices of all specimens (see Figures 6a - 13a).

(ix) A small amount of foreign phase was present in all batches of fuel material. This phase was relatively light in colour and was assumed to be a carbide (for example, UC - ThC solution or UC - UO - ThC solution) resulting from contamination from the hot pressing die.

Before irradiation the dimensions of all specimens were measured with a vernier micrometer to an accuracy of ± 0.00025 cm. Densities measured by liquid displacement were not reproducible because of the effects of porosity and these results are not reported. Specimens were also photographed before being sealed into the irradiation or heat treatment cans.

2.3 Rig Design and Assembly

The specimens were irradiated in HIFAR in a four inch vertical hole (the 4V-5 hole) using a standard A.A.E.C. 4V fuel rig. Rigs of this type rely on nuclear heating alone to provide the design specimen temperatures and are cooled by the reactor heavy water.

The general arrangement of the rig is shown in Figure 1. It consisted of two side-by-side aluminium formers which dipped into the reactor heavy water and were protected by a perforated outer aluminium tube. Eight full specimens held in graphite carriers and canned in stainless steel were loaded into each former so that duplicate specimens occupied equivalent positions in each stringer. A schematic cross section of portion of a stringer showing the graphite carrier, stainless steel can and aluminium former is shown in Figure 2. The stainless steel can was a push fit in the aluminium former which in turn was a push fit in the aluminium outer tube.

In this experiment, only one thermocouple was used for each specimen can. All drilled specimens were loaded into stringer B as the lower halves of the twin specimens and the thermocouple pockets on the lower end caps extended into the holes. In stringer A, thermocouples were set into recesses in the lower ends of the graphite carriers. The width of the gas gap between the stainless steel cans and the graphite carriers was chosen so that, when filled with helium, nuclear heating would raise the specimen temperature to the desired value during operation. The heat output of each specimen was calculated using flux data for a simulated 4V rig obtained during low power operation of HIFAR (Connolly and McKenzie 1961); flux depressions in the specimens were

calculated by the empirical method due to Lewis (1955). Individual heat-transfer calculations to arrive at the gas-gap dimensions were made for each can assuming that heat was lost only by conduction and radiation across the gap and using temperature distribution data obtained in tests on a prototype out-of-pile rig.

The specimens were held firmly by the graphite carriers which were held centrally in the stainless steel can by the thermocouple pockets on the end-caps. Cobalt flux monitors in alumina sheaths were wired to the thermocouple pockets on the lower end caps.

The cans were filled with pure helium and the end caps welded to the cans in a helium-filled dry box. After leak testing the cans were fitted with thermocouples, assembled into stringers, and loaded into the rig. All thermocouples were mineral-insulated and stainless-steel sheathed. They were checked against a standard at 500°C before use and found to be within ± 2°C of the correct value.

The whole assembly was finally attached to a shield plug (Figure 1) provided with service tubes and purge lines (to purge the space between the specimen cans and the formers). Thermocouples were connected to compensating leads at the top of the plug and the temperatures of all thermocouples recorded on multipoint, potentiometric instruments.

2.4 Rig Operation

After loading the rig into the reactor the space between the specimen can and the aluminium former was purged with helium and pressurised to 1 p.s.i. above atmospheric.

In the first approach to power, the power level was raised in steps of 2 MW until 10 MW was reached. At this stage the temperatures of all specimens in stringer B were above the design minimum of 600°C and specimen 126/129 exceeded the designed upper limit of 800°C. As repeated purging with helium failed to reduce the temperatures the reactor was shut down and the rig rotated so that both stringers lay on the one radius from the core centre. With this orientation the temperatures in stringer B fell owing to the shielding effect of stringer A but specimen 126/129 could not be brought lower than 840°C. However it fell steadily during irradiation and was below 800°C at the start of the second operating period.

Power levels did not exceed 10.2 MW and the general behaviour of the rig was steady. However, several marked temperature drifts occurred in stringer A specimens during the first operating period. These charges occurred between 100 and 400 hours and the rate of drift was steady. Specimens 100/101 and 112/113 fell in temperature at about 1°C per hour and specimens 118/119, 130/131, and 148/149 rose in temperature at about ½°C per hour. No explanation was found for this behaviour and little importance was attached to it for, as discussed in Section 2.5, the record of temperature in stringer A was not considered accurate.

Temperature history charts for both stringers are presented in Figure 3a and b. In general all specimens showed a steady fall during irradiation although discontinuous rises or falls were usually noted at each start-up. These did not appear to be due to differences in reactor power and the true cause is not known. The steady falls in temperature are attributed to depletion of U235 content of the specimens and the consequent decrease in fission rate.

The rig was in the reactor for 3550 hours during which time there were six scheduled shut-downs of two to three days, one unscheduled shut-down of about 24 hours duration and nine trips of 2 – 4 hours each. At each trip or shut-down the specimen temperatures fell to approximately 40°C at a rate of 60 – 80°C per minute.

2.5 Irradiation Temperatures

The true centre-temperatures of irradiation specimens should be indicated correctly by thermocouples extending to the specimen centres. Thus, the true specimen temperatures in stringer B were taken to be those indicated on the recording equipment. However, stringer A centre temperatures were not directly indicated and had to be estimated from temperature records. These showed that rotation of the rig at the initial reactor start-up lowered the temperatures of stringer B specimens but had no significant effect on those in stringer A. Thus, an estimate – considered to be reasonably accurate – of the mean centre temperatures in stringer A was obtained by adding the mean indicated centre temper-

ature of the appropriate stringer B specimen and the drop in that temperature observed on rotating the rig from its initial to final positions.

The estimated mean temperatures for all specimens are listed in Table 3, those for stringer A being obtained as described above and those for stringer B being the weighted means of the indicated temperatures. The range limits of the operating temperatures for stringer B and the temperature drops due to rotation of the rig are also given.

2.6 Post-Irradiation Examination

At the end of the irradiation period, the rig was unloaded and stored for several weeks in the HIFAR storage block. It was dismantled in the high activity handling cells by cutting open the outer aluminium tube and withdrawing the specimen cans from the formers.

The amounts of fission gas released during irradiation were measured by piercing the cans in an evacuated system of known volume and measuring the pressure rise. Gas compositions were determined by mass-spectrometry.

After the specimens were recovered from the cans the surfaces were examined and photographed at magnifications of 2 – 15 times using a stereo-periscope. Dimensions were measured using a dial gauge in conjunction with slip gauges. Volumes and densities were determined from dimensions.

The half-specimens having thermocouple pockets (that is, numbers 105, 111, 117, 123, 129, 135, 147, and 153) were slit into longitudinal and transverse sections and examined metallographically. Metallographic control samples of as-fabricated and heat treated unirradiated material equivalent to specimens 117 and 135 were prepared together with the irradiated specimens. These samples provided a means of comparing the remote metallographic preparation with that done in the inactive laboratory on unirradiated specimens. The polishing techniques involved grinding on 120, 220, 320, 400, and 600 grade silicon carbide papers on a Buehler Automet machine followed by polishing for 48 hours on a "Syntron" vibratory polishing machine using a nylon cloth and medium grade alumina compound.

Four different etchants, 10 per cent. ammonium bifluoride, phosphoric acid, 1:1 hydrofluoric acid, and a hot aqueous solution of H_2SO_4 (10%) and H_2O_2 (20 v/o) were used on specimens 135 and 147 in an attempt to reveal the zones surrounding the fuel particles which were damaged by fission fragment recoil.

The burn-up in each specimen was calculated from HIFAR flux data (obtained from measurements made during low power operation, Connolly and McKenzie 1960) and from fluxes calculated from the gamma activities of cobalt monitors. In each case flux depressions in the specimens were estimated by the empirical method developed by Lewis (1955). Chemical checks on the burn-ups of specimens 117 and 123 were made by radiochemical determination of the Cs-137 yield and mass-spectrometer determination of the U-235 : U-238 ratio.

Thermal stresses were calculated for all specimens using the method described in the appendix.

Fracture surfaces of specimens 135, 148 and as-fabricated samples of the same hot-pressed compacts were examined with the electron microscope. Two-stage negative cellulose acetate-carbon replicas shadowed with Pt – Pd were used.

2.7 Out-of-Pile Control Specimens

One specimen from each group defined in Table 1 was sealed in a graphite carrier and stainless steel can in the same manner as the irradiation specimens. They were subjected to a heat treatment which followed all but the minor variations (less than 20 °C) in the thermal histories of the corresponding specimens in stringer B of the irradiation rig. On completion of the heat treatment the specimens were examined for dimension and density changes. Dimensions were measured with a vernier micrometer both before and after heat treatment. Only specimens 115 and 133 were examined by metallography. By remote control they were polished, examined, and photographed with the irradiated specimens.

3. RESULTS

3.1 Burn-Up Determination

A full comparison of burn-up results is given in Table 4. Burn-ups are expressed as atomic

per cent. uranium for the four methods used and also as atomic per cent. heavy metals and equivalent burn-up for the method using tabulated fluxes. Fission densities for whole specimens and for fuel material alone are also included in the table.

The chemical determinations of burn-up, which should be the most accurate, agree reasonably well with the burn-ups calculated from tabulated fluxes, although they are, in general, a little high. The burn-ups calculated from fluxes measured with cobalt monitors are consistently low. No explanation can be offered for this as good agreement has generally been found in other rigs. Burn-ups calculated from tabulated fluxes have been used for calculating percentage releases of fission gases, fission densities, and thermal stresses. In making these calculations, however, the fluxes for stringer B specimens were reduced with respect to stringer A fluxes according to the fractional differences between the monitored fluxes for the two stringers. Thus, account was taken of the shielding of stringer B due to the radial alignment of stringers during irradiation. (The differences, expressed as fractions of stringer A values are given in Table 4).

3.2 Fission Gas Release

Successful gas sampling was achieved with all specimen cans. The quantities of fission gases released from the specimens are given in Table 5. These are quoted as actual quantities of each isotope found in each can and as percentages released into the can of the total quantity of each isotope produced in the specimens.

The release of gas from all specimens was very low; the highest percentage for any isotope was 0.5 per cent. and the mean percentage release was 0.19 per cent.

The release of gas from specimens 118/119 in can A6 (6.25×10^{-3} cm^3) was greater than expected from the average releases while that from specimens 120/123 in can B6 (2.81×10^{-3} cm^3) was lower than expected. The low release for can B6 is not readily explained but the high release for can A6 was probably due in part to the high swelling (1.24 per cent.) of specimen 119.

3.3 Macroexamination

Macroexamination failed to show any changes in surface condition resulting from irradiation. No distortion, discoloration, cracking, or pitting could be observed in any of the specimens.

The heat treated control specimens likewise showed no surface changes with the exception of 103 which was chipped at the corners and extensively cracked.

3.4 Dimension and Volume Changes

The pre- and post-irradiation dimensions are shown in Table 6. The dimension changes were never greater than 0.5 per cent. and were generally less than 0.3 per cent. The accuracy of the measurements is thought to be ± 0.1 per cent.

Volume changes calculated from dimension changes are also given in Table 6. Specimens containing coarse fuel grains increased in volume by an average of 0.6 per cent. The swelling of individual specimens varied randomly and did not correlate to temperature or fission density. The mean swelling in specimens containing fine fuel grains was 0.97 per cent.

Dimensions of unirradiated control specimens are given in Table 7. The only specimen to show any perceptible change in dimensions after heat treatment was number 103. As mentioned in Section 3.3, this specimen was extensively cracked. The reason for the cracking could not be ascertained.

3.5 Metallographic Examination

The observations made during the examination of microstructures can be summarised as follows:

(i) The fuel particles showed no changes from the unirradiated condition even at magnifications of 600.

(ii) After irradiation the small rounded pores in the BeO matrix were supplemented by larger angular pores. The larger pores were more abundant in specimens of high fission concentration (that

is, fissions per unit volume of total specimens) and were most noticeable at concentrations of 6×10^{19} fissions cm^{-3} and above (specimens 135, 117, 147, 123, and 129) although specimen 105 (only 2×10^{19} fissions cm^{-3}) was also very pitted.

(iii) The angular pores described in (ii) were of the same shape and size as the grains of the BeO matrix and were gradually eliminated by extended final stage polishing (see Figure 13). They appear, therefore, to result from tear-out of grains during the coarse stages of metallographic preparation.

(iv) The apparent increase in porosity described in (ii) was not observed in unirradiated control specimens (either as-fabricated or heat-treated) polished together with their irradiated counterparts. (See Figures 5 – 13).

(v) The microstructures of unirradiated heat-treated control specimens showed no changes from the as-fabricated condition. Microstructures of specimens 115 and 133 are given in Figure 15 and the as-fabricated microstructures in Figures 7a and 10a respectively.

(vi) The only effect of the four etchants was to emphasise grain boundaries in the BeO matrix. In no case, even that of highest burn-up, did the matrix immediately surrounding the fuel grains show different etching characteristics to the bulk of the BeO matrix.

The zones of damage around fuel grains observed by Yeniscavich and Bleiberg (1960) resulted from fission concentrations of 11×10^{20} fissions cm^{-3} of specimen. Johnson and Tobin (1960) found no evidence of damaged zones at fission concentrations of 2.4×10^{20} fissions cm^{-3} and so it is not surprising that none were found in this experiment where the maximum fission concentration was only 1.5×10^{20} fissions cm^{-3}.

Examination of fracture surfaces with the electron microscope showed that fracture was predominantly intergranular on irradiation. Fractographs of specimen 148 and its as-fabricated control specimen are shown in Figures 15 and 16. Distinguishing the fuel grains from the matrix proved to be impossible on both the unirradiated and irradiated specimens although optical examination showed numerous fuel grains at the fractured surface.

4. DISCUSSION

The results described in this report suggest that fission product damage should not result in serious deterioration of UO_2–ThO_2–BeO fuels at the burn-ups envisaged for the H.T.G.C. system. The dimensional stability was very good and there was no evidence of radial cracking even though thermal stresses were estimated to reach high values (up to 30,000 p.s.i.) in some specimens. Although several assumptions had to be made in calculating these thermal stresses it is thought the assumptions would tend to give a low value; particularly the assumption that the thermal conductivity is unaltered by irradiation. The fission product gas retention was also very satisfactory, the amount escaping being of the same order as would be expected to recoil from fuel particles at the surface of the fuel specimens, that is, very little escape by bulk diffusion or diffusion along pores had occurred.

The results did not provide conclusive evidence of the superiority of coarse fuel particles over fine fuel particles although the former did give smaller dimension changes. However some preliminary x-ray examination (Hanna et al. 1962) showed that broadening of the BeO reflections occurred and was much more severe in the fine grain than in the coarse grain material; this broadening indicates that the BeO matrix was in a state of strain. More marked differences would probably become apparent at higher burn-ups. Studies are in progress to investigate further the effect of fuel-particle size.

Apart from the broadening of the BeO x-ray reflections noted above, the only deleterious effect of irradiation noted in this experiment was the greater ease of "tear-out" of grains in the irradiated specimens during grinding for metallographic examination. It is very probable that these two effects are related; the state of strain indicated by the x-ray work could well cause weakening of the grain boundaries. The cause of this strain is not immediately apparent. The uniformity of the effect along specimen radii rules out thermal stress as the predominant cause. Other possibilities which should be considered are (i) swelling of fuel grains, (ii) lattice damage due to fast neutrons born in the specimens (iii) helium production by the (n, 2n) and (n, α) reactions of the beryllium nucleus, and (iv) fission product damage due to non-ideal shape of fuel particles.

Although Yeniscavich and Bleiberg made no reference to grain tear-out or apparent porosity increases in matrices of their UO_2-BeO specimens, their photomicrographs suggest that tear-out did occur. They did report cracks in the matrices (which were probably manifestations of the same phenomenon) and attributed them to stresses generated by the swelling of fuel grains. Although no fuel grain swelling was obvious in this experiment and the fission density in the fuel was below that at which catastrophic swelling of bulk UO_2 occurs, there may have been sufficient to cause some strain.

The integrated fast flux from the reactor to which the specimens were subjected was less than 10^{18} nvt which would produce no effects in BeO. However, the fast neutrons resulting from fissions within the specimens could cause an effect and Lawrence (A.A.E.C. report in preparation) has used an IBM-1620 programme to analyse the nuclear interaction and escape of fission neutrons born in the specimens during this experiment. The primary collision densities evaluated from his results lie between 1.5×10^{19} and 9×10^{19} collisions per cm^3 of specimen depending on specimen composition. From the results of Hickman, Sabine, and Coyle (1962) on hot-pressed beryllium oxide irradiated with fission neutrons, one can interpolate that primary collision densities in this range will cause an increase of 0.03 to 0.15 per cent. in the c parameter and little or no change in the a parameter. These values were deduced from pile temperature irradiation results and allow for the fact that parameter changes observed after irradiation at 500 to 700 °C are 3 to 5 times lower than the changes at pile temperature (75 to 100 °C).

The helium content of the BeO in the fuel specimens of this experiment can be evaluated from the product of the primary collision density and the ratio of the effective absorption cross section for a fission spectrum * to the scattering cross section. In specimens 124/125 and 126/129 where fission density was greatest, the helium content was 0.33 cm^3 per cm^3 of BeO The calculations of Lawrence lead to a helium content of about 0.24 cm^3 per cm^3 of BeO so the above value may be regarded as an upper limit for all specimens. Hickman (1962 b) has observed that 0.5 cm^3 of helium per cm^3 of BeO has no effect in irradiation at below 700 °C and it is unlikely therefore that helium generation has led to any significant effects in this experiment.

The fraction of matrix damaged increases with the surface area of the fuel phase and irregular fuel grains will therefore cause more matrix damage than the spheres of the theoretical model. However, the results have shown that the behaviour of specimens containing 0 - 50 micron fuel particles is only slightly inferior to that of specimens containing 100 to 180 micron particles. Thus, the comparatively small difference in surface area between coarse spherical and coarse irregular fuel particles is not likely to produce a significant deterioration in irradiation stability, at least under the conditions of this experiment.

It would appear therefore, that the strain in the beryllium oxide matrix must be due to fast neutron displacement damage resulting from neutrons born in the specimens or from swelling of the fuel grains.

5. CONCLUSIONS

The experiment has shown that at equivalent burn-ups of up to about 250 per cent. (1.4×10^{20} fissions cm^{-3}) at 600 to 850 °C, dispersions of $(UTh)O_2$, in beryllium oxide have,

(i) excellent capacity for retaining fission gas;

(ii) good dimensional stability; and

(iii) good integrity and resistance to high thermal stresses.

However, metallographic examination revealed an apparent weakening of the beryllium oxide along the grain boundaries. This effect was uniform throughout the specimens, and could be due to fast neutron damage resulting from neutrons born in the specimens or to swelling of fuel particles.

---

* The effective absorption cross section was taken as 0.125 barns being the sum of 0.100 barns for the (n, 2n) reaction and 0.025 barns for the (n, α) reaction. Each reaction was assumed to yield two helium atoms.

Specimens containing fuel grains of about 10 micron diameter behaved similarly in most respects to specimens containing fuel grains in the 100 – 180 micron range. However, their dimensional stability was slightly inferior and preliminary x–ray data suggest that there is considerably more matrix damage in the second case.

Further examination of specimens by x–ray diffraction, compression testing, and electron microscopy is to be done and will be reported.

It should be emphasised that the primary aim of this experiment was to investigate fission product damage and although some fast neutron damage to the matrix occurred, much higher fast neutron damage will be encountered in an actual reactor fuel element. Results on matrix damage and on fuels irradiated in a high fast neutron flux are therefore required before a full evaluation of this fuel material can be made.

6. ACKNOWLEDGMENTS

Many members of the Lucas Heights staff contributed to this experiment. Acknowledgment is due to Operations Division for the design and operation of the rig, members of the Irradiation Group for assembly and testing of the rig, the Ceramics Group for the provision of specimens, the Analytical Chemistry Section for fission gas analysis and chemical burn–up determination, Chemistry Section for dissolution of samples for burn–up determination, Mr. B.R. Lawrence for nuclear calculations, and members of the Hot Cell Group, particularly Mr. J. Mellor, for the post–irradiation examination.

7. REFERENCES

Connolly, J.W., and McKenzie, C.D. (1960). – AAEC/TM64.

Hanna, G.L., Hickman, B.S., and Hilditch, R.J. (1962). – AAEC/E96.

Hickman, B.S. (1958). – Internal report AAEC/K181.

Hickman, B.S. (1962a). – AAEC/TM139.

Hickman, B.S. (1962b). – AAEC/E99.

Hickman, B.S., Sabine, T.M., and Coyle, R.A. (1962). – J. Nuc. Mat. 6: 190.

Johnson, D.E., and Tobin, J.M. (1960). – TID–7602 Pt. 1.

Lewis, W.B. (1955). – Nucleonics 12 (10): 31.

Reeve, K.D. and Ramm, E.J. (1960). – AAEC/TM51.

Weber, C.E. (1959). – Progress in Nuclear Energy, Series V, Vol. 2 p. 295.

White, D.W., Beard, A.P., Willis, A.H. (1957). – KAPL–1909.

Yeniscavich, W., and Bleiberg, M.L. (1960). – WAPD–BT–20.

APPENDIX 1

THERMAL STRESS CALCULATIONS

1. Notation

E	elastic modulus
F	ratio of neutron flux at surface to undisturbed flux
H	heat rating
k_{BeO}	thermal conductivity of BeO
k_d	thermal conductivity of dispersion
k_{UThO_2}	thermal conductivity of $(UTh)O_2$
R	ratio of k_{BeO} to k_{UThO_2}
M	weight of U–235 in specimen
N	number of fissions/second/watt
P_c	probability of neutron capture in specimen
Q	heat output of specimen
r	specimen radius
V	specimen volume
V_f	volume fraction of fuel phase
α	coefficient of thermal expansion
μ	Poisson's ratio
ϕ	thermal neutron flux
σ_t	tangential stress at specimen surface

2. Formulae and Values

Thermal stresses at specimen surfaces were calculated from the following expression:

$$\sigma_t = \frac{E\,\alpha}{1-\mu} \cdot \frac{H\,r^2}{8\,k_d}$$

Because of insufficient data on dispersion systems, it was assumed that elastic modulus, coefficient of expansion, and Poisson's ratio of dispersions were the same as those for beryllium oxide in the temperature range involved. The values used were:

Elastic modulus	41.25×10^{-6} p.s.i.
Coefficient of expansion	$10.7 \times 10^{-6} \cdot {}^{\circ}C^{-1}$
Poisson's ratio	0.31

Heat ratings were calculated from the formula:

$$H = \frac{Q}{V} = \frac{P_c\,F\,\phi\,S}{4\,N\,V}$$

APPENDIX 1 (continued)

which, for small cylinders, reduces to

$$H = \frac{(4.11 \times 10^{-11})\,\phi M}{V}$$

Thermal conductivities of dispersions are sensitive to $(U\,Th)O_2$ content. Conductivities for the several compositions were calculated from the formula

$$k_d = k_{BeO} \cdot \frac{1 + 2\,V_f\,\frac{(1-R)}{(2R+1)}}{1 - V_f\,\frac{(1-R)}{(2R+1)}}$$

which was adapted from Euken's expression (1932) for porous bodies. Heuer et al. (1962) have shown that this holds, at low temperatures at least, for $(UTh)O_2$–BeO bodies.

The values of thermal conductivities used in the calculations are tabulated below.

Temperature °C	k_{BeO} W cm^{-1} (deg. C)$^{-1}$ sec^{-1}	$k_{U\,ThO_2}$ W cm^{-1} (deg. C)$^{-1}$ sec^{-1}	$R\left(\frac{k_{BeO}}{k_{U\,ThO_2}}\right)$
600	0.46	0.04	11.5
700	0.33	0.03	11
800	0.27	0.03	9

3. References

Euken, A. (1932). – Ceram. Abst. 11 (11) : 576.

Heuer, P., Stolarski, G., and Pryor, A. (1962). – AAEC Internal note MP/TN 4.

TABLE 1

SPECIMEN COMPOSITIONS

Specimen Number	Basic Atom Ratio U : Th : Be	Accelerated Atom Ratio U : Th : Be	Composition W/O (Actual)			Volume Per cent. $(U,Th)O_2$	$(U,Th)O_2$ Particle Size (microns)	Volume Per cent. of Matrix Damaged by Recoil (Theoretical)
			UO_2	ThO_2	BeO			
100/101 102/105	1 : 30 : 3000	8 : 23 : 3000	2.6	6.8	90.5	3.0	100 – 185	3.1
106/107 108/111	1 : 30 : 2000	8 : 23 : 2000	3.7	9.7	86.3	4.4	" "	3.3
112/113 114/117	1 : 30 : 1000	8 : 23 : 1000	6.7	17.4	75.9	8.4	" "	7.2
118/119 120/123	1 : 30 : 500	8 : 23 : 500	10.9	28.3	60.9	15.7	" "	14.7
124/125 126/129	1 : 30 : 250	8 : 23 : 250	15.2	39.4	45.4	25.8	" "	27.5
130/131 132/135	1 : 30 : 2000	16 : 15 : 2000	7.4	7.7	84.9	4.4	" "	3.3
139/140 141/147	1 : 30 : 2000	25 : 6 : 2000	11.9	2.8	85.3	4.4	" "	3.3
148/149 150/153	1 : 30 : 2000	8 : 23 : 2000	3.7	10.1	86.1	4.4	< 10	100

TABLE 2

DIMENSIONS OF COARSE FUEL GRAINS

Composition	Length Microns			Breadth Microns			Number of Particles Examined
	Max.	Min.	Mean	Max.	Min.	Mean	
8U : 23Th	280	84	167	196	56	84	50
25U : 6Th	420	63	174	105	21	86	20
16U : 15Th	224	70	134	105	28	65	10

TABLE 3

IRRADIATION TEMPERATURES, THERMAL STRESSES AND HEAT RATINGS

Specimen	Stringer and Position	Temperature Drop due to Repositioning of Rig °C	Mean Irradiation Temperature °C	Irradiation Temperature Range, Stringer B °C	Heat Rating watts cm^{-3}	Thermal Stress p.s.i.
100/101	A 3		655		65	3500
102/105	B 3	45	610	570 – 670	54	2700
106/107	A 4		675		99	5800
108/111	B 4	65	610	600 – 650	76	3800
112/113	A 5		745		194	15800
114/117	B 5	95	650	640 – 700	158	9500
118/119	A 6		695		300	9100
120/123	B 6	75	620	600 – 650	256	8300
124/125	A 2		820		415	31000
126/129	B 2	100	750	720 – 835	345	19600
130/131	A 7		765		168	12700
132/135	B 7	75	690	670 – 730	148	9200
139/140	A 1		735		225	15900
141/147	B 1	65	670	640 – 690	205	12000
148/149	A 8		630		89	4750
150/153	B 8	30	600	580 – 630	80	3850

TABLE 4

BURN-UP VALUES

Specimen No.	Stringer	From Tabulated Fluxes			From Monitored Fluxes		From Cs-137 Yield	From U^{235}/U^{238}	Fission Density	
		a/o U (A)	a/o Heavy Metals	Equivalent Burn-up %	a/o U (B)	Fractional Difference $\left(\frac{A-B}{A}\right)$	a/o U	a/o U	Whole Specimen Fissions $cm^{-3} \times 10^{-19 \text{ or } 20}$	Fuel Only Fissions $cm^{-3} \times 10^{-19 \text{ or } 20}$
100/101	A	13.0	3.4	104	9.8	.11			2	7.5
102/105	B				8.7					
106/107	A	13.4	3.5	107	11.7	.17			3.5	8
108/111	B				9.7					
112/113	A	13.0	3.4	104	10.7	.13			6.5	7.5
114/117	B				9.3		13.4	14.5		
118/119	A	11.6	3.0	93	9.2	(.09)*			10	6.5
120/123	B				–		13.4	12.4		
124/125	A	9.4	2.4	75	6.4	.06			15	6
126/129	B				6.0					
130/131	A	11.8	6.1	188	–	(.06)*			6	14
132/135	B				8.2					
139/140	A	9.3	7.5	230	6.3	.05			8	18
141/147	B				6.0					
148/149	A	11.8	3.1	94	9.7	.04			3	7
150/153	B				9.3					

* Interpolated Values

TABLE 5

FISSION PRODUCT GAS RELEASE

Specimen	Volume of Gas Released, $cm^3 \times 10^{-5}$								Percentage of Total Gas Released							
	Krypton			Xenon				Total	Krypton			Xenon				Mean
	83	84	86	131	132	134	136		83	84	86	131	132	134	136	
100/101	2	4	8	11	19	36	53	133	0.2	0.2	0.2	0.2	0.25	0.25	0.45	0.25
102/105	2	4	9	10	17	33	47	122	0.25	0.25	0.3	0.2	0.25	0.25	0.45	0.28
106/107	1	1	5	7	11	21	32	78	0.1	0.05	0.1	0.1	0.1	0.1	0.15	0.1
108/111	1	2	4	7	10	23	31	78	0.1	0.1	0.1	0.1	0.1	0.1	0.2	0.1
112/113	4	6	11	15	23	46	61	166	0.1	0.1	0.1	0.1	0.1	0.1	0.15	0.1
114/117	4	6	13	19	25	50	69	186	0.15	0.1	0.1	0.1	0.1	0.1	0.2	0.12
118/119	11	25	53	53	88	164	231	625	0.3	0.4	0.4	0.3	0.3	0.3	0.6	0.37
120/123*	4	9	20	27	41	75	105	281	–	–	–	–	–	–	–	–
124/125	11	21	46	48	80	140	114	460	0.3	0.3	0.3	0.2	0.25	0.25	0.25	0.26
126/129	4	8	21	27	42	80	107	289	0.1	0.1	0.2	0.15	0.15	0.15	0.25	0.16
130/131*	1	4	8	11	20	39	55	138	–	–	–	–	–	–	–	–
132/135	2	5	9	11	17	33	46	123	0.1	0.1	0.1	0.1	0.1	0.1	0.14	0.1
139/140	8	15	34	42	67	126	170	462	0.2	0.2	0.25	0.2	0.25	0.25	0.4	0.25
141/147	8	11	23	31	50	93	126	342	0.25	0.2	0.2	0.2	0.2	0.2	0.35	0.23
148/149	2	2	5	6	9	20	31	75	0.1	0.1	0.1	0.1	0.1	0.1	0.2	0.1
150/153	1	2	4	8	13	25	38	91	0.1	0.1	0.1	0.1	0.1	0.1	0.2	0.1

* Burn–up not known accurately.

TABLE 6

DIMENSION AND VOLUME CHANGES OF IRRADIATED SPECIMENS

Specimen	Diameter			Length			Volume Increase %	Mean Volume Increase %
	Before cm	After cm	Increase %	Before cm	After cm	Increase %		
100	0.965	0.968	0.3	1.451	1.454	0.25	0.85	0.7
101	0.966	0.968	0.2	1.454	1.456	0.15	0.55	0.7
102	0.963	0.965	0.2	1.455	1.457	0.15	0.55	0.60
105	0.964	0.967	0.25	1.451	1.453	0.15	0.65	
106	0.966	0.967	0.1	1.440	1.441	0.05	0.25	0.37
107	0.965	0.967	0.2	1.442	1.443	0.10	0.50	
108	0.965	0.966	0.15	1.447	1.449	0.15	0.45	0.40
111	0.964	0.965	0.15	1.449	1.450	0.05	0.35	
112	0.965	0.966	0.1	1.449	1.459	0.7	0.9	
113	0.965	0.965	–	1.456	1.451	–0.3	–	–
114	0.965	0.967	0.2	1.455	1.457	0.15	0.55	0.6
117	0.965	0.967	0.2	1.452	1.455	0.25	0.65	
118	0.722	0.722	–	1.445	1.449	0.25	0.25	0.65
119	0.723	0.725	0.3	1.446	1.453	0.5	1.05	
120	0.723	0.724	0.05	1.447	1.451	0.25	0.35	0.4
123	0.723	0.723	0.05	1.445	1.450	0.35	0.45	
124	0.725	0.7255	0.1	1.447	1.450	0.15	0.30	0.5
125	0.725	0.7265	0.2	1.447	1.451	0.25	0.65	
126	0.720	0.720	–	1.449	1.452	0.15	0.15	0.3
129	0.722	0.723	0.15	1.451	1.454	0.2	0.50	
130	0.966	0.967	0.15	1.446	1.448	0.15	0.45	0.5
131	0.965	0.967	0.20	1.449	1.452	0.15	0.55	
132	0.965	0.968	0.3	1.449	1.452	0.2	0.8	0.8
135	0.965	0.968	0.3	1.450	1.453	0.2	0.8	
139	0.964	0.967	0.3	1.450	1.454	0.25	0.85	0.75
140	0.966	0.968	0.2	1.448	1.452	0.25	0.65	
141	0.964	0.966	0.2	1.450	1.453	0.15	0.55	0.7
147	0.965	0.968	0.3	1.452	1.455	0.20	0.85	
148 *	0.965	0.969	0.4	1.445	1.447	0.15	0.95	0.9
149	0.965	0.968	0.35	1.454	1.456	0.15	0.85	
150 *	0.964	0.968	0.4	1.439	1.443	0.25	1.05	
153	0.966	0.971	0.5	1.446	1.449	0.20	1.10	1.1

* 0 – 50 micron fuel grains.

TABLE 7

DIMENSION CHANGES IN HEAT TREATED CONTROL SPECIMENS

Specimen Number	Corresponding In–pile Specimen	Diameter (cm)			Length (cm)			% Change in Volume
		Before	After	% Change	Before	After	% Change	
103	102/105	0.965	0.966	+0.1	1.457	1.467	+0.7	+0.9
109	108/111	0.965	0.965	–	1.448	1.447	–	–
115	114/117	0.965	0.965	–	1.452	1.452	–	–
121	120/123	0.723	0.723	–	1.448	1.448	–	–
127	126/129	0.723	0.723	–	1.449	1.450	–	–
133	132/135	0.966	0.965	–	1.448	1.448	–	–
143	141/147	0.967	0.965	–	1.453	1.453	–	–
151*	150/153	0.965	0.965	–	1.451	1.451	–	–

* 0 – 50 micron fuel grains.

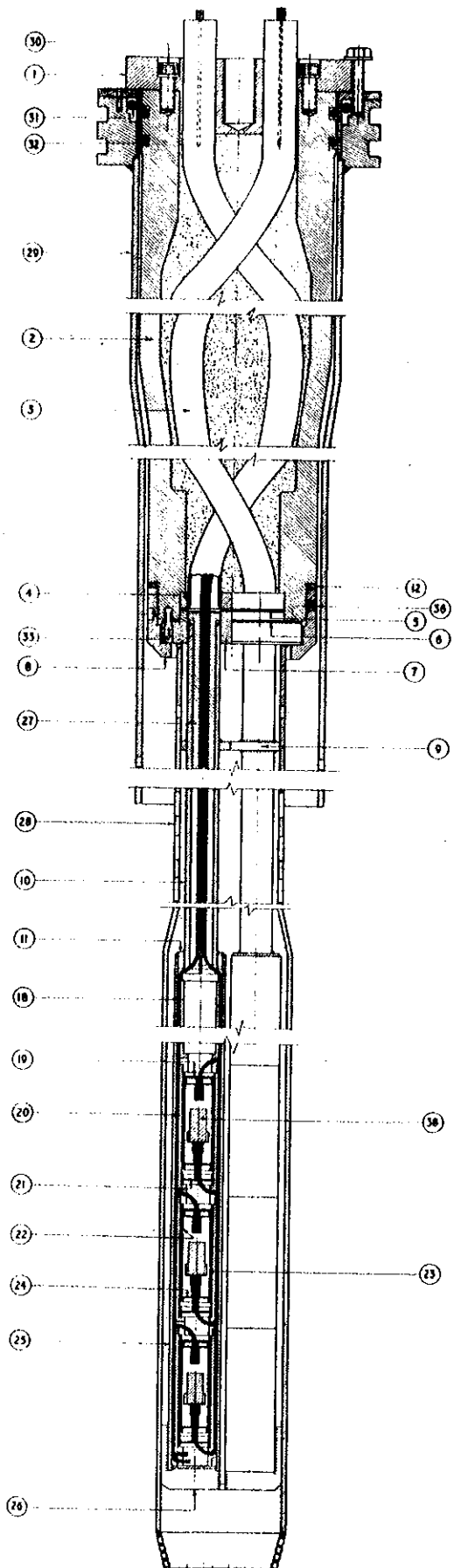

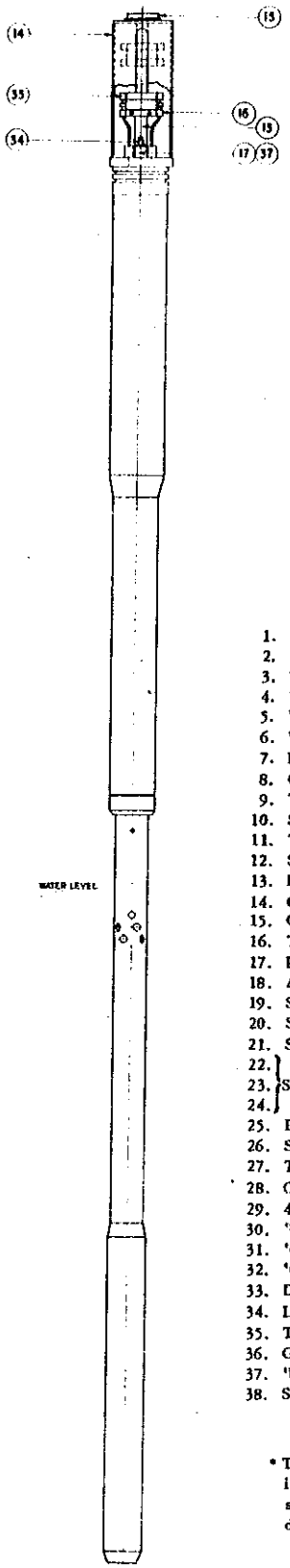

1. Top Plate
2. Plug
3. Through Plug Tubes
4. Tube Locating Plate
5. Washer
6. Washer
7. Locating Plate
8. Clamping Ring
9. Tube Guide
10. Spacer Tube
11. Tube Reducer
12. Sealing Washer
13. Lifting Bolt and Terminal Block Holder
14. Cover
15. Clamping Nut
16. Thermocouple Clamping Plate
17. Purging Tube Adaptor
18. Aluminium Former
19. Stainless Steel Can End
20. Stainless Steel Can
21. Stainless Steel Can End
22. } Specimen Capsule* Components
23. }
24. }
25. Experimental Former
26. Spacing Fins
27. Thermocouple Former
28. Outer Casing
29. 4V Thimble
30. 'Unbrako' Capscrews
31. 'O' Ring
32. 'O' Ring
33. Dowel
34. Lockheed Coupling
35. Terminal Blocks
36. Grubscrew
37. 'Unbrako' Screws
38. Specimen

* The capsule shown is for irradiation of metallic fuel specimens. Figure 2 shows details of ceramic fuel capsule.

FIGURE 1 GENERAL ARRANGEMENT OF THE 4V RIG FOR IRRADIATING FUEL SPECIMENS

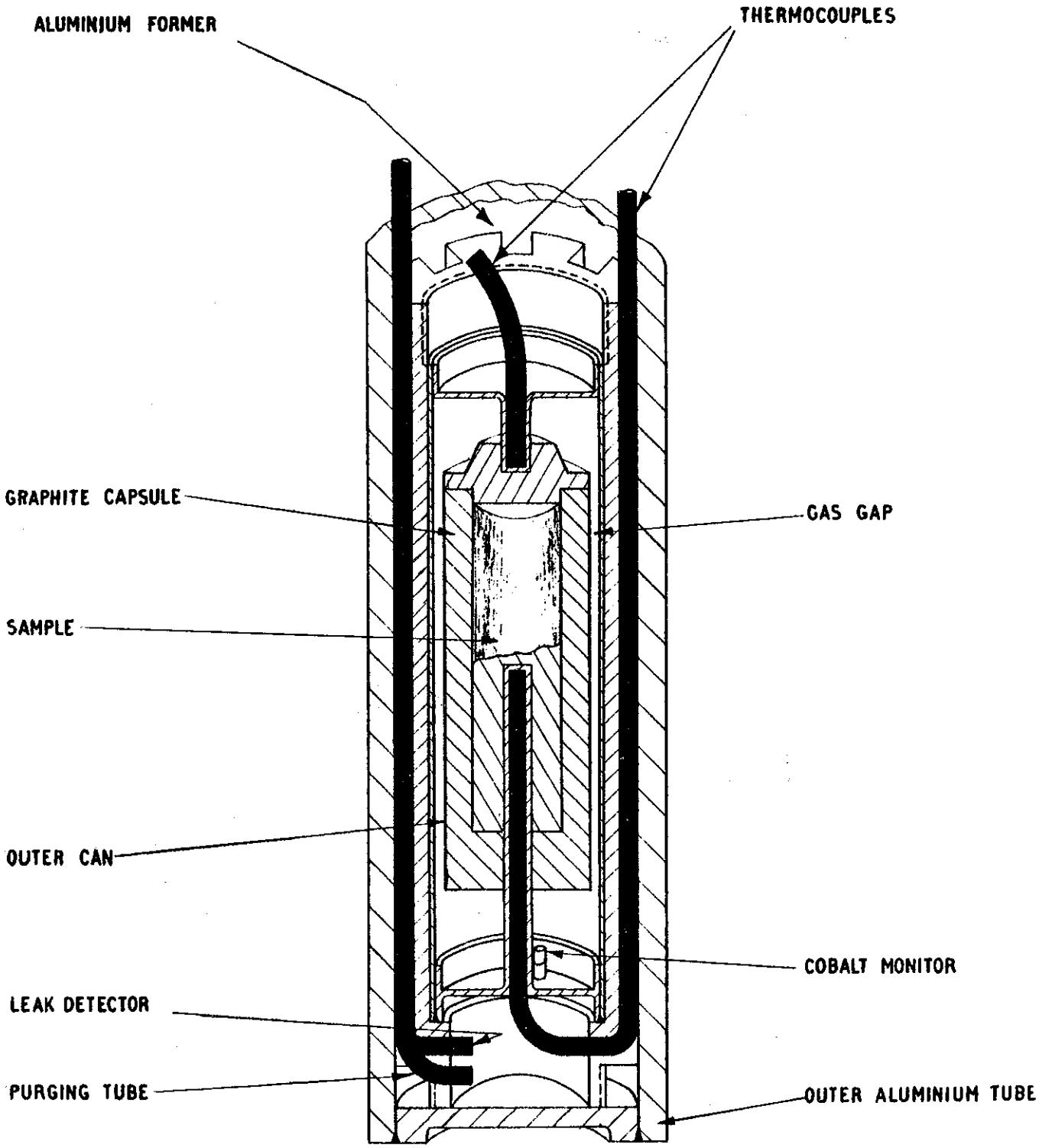

FIGURE 2 SCHEMATIC CROSS-SECTION OF SPECIMEN IRRADIATION CAPSULE

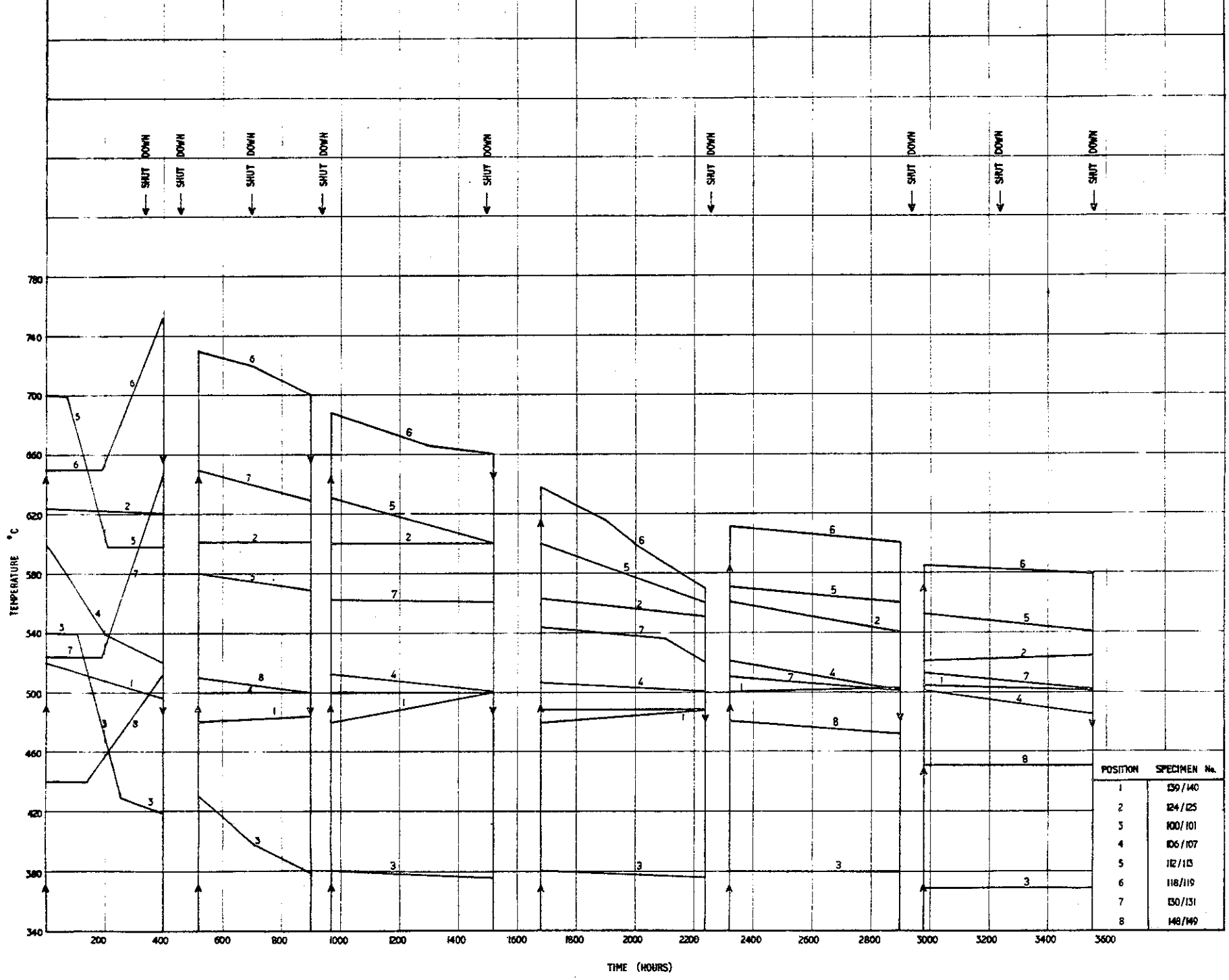

FIGURE 3a SPECIMEN TEMPERATURE CHART STRINGER A

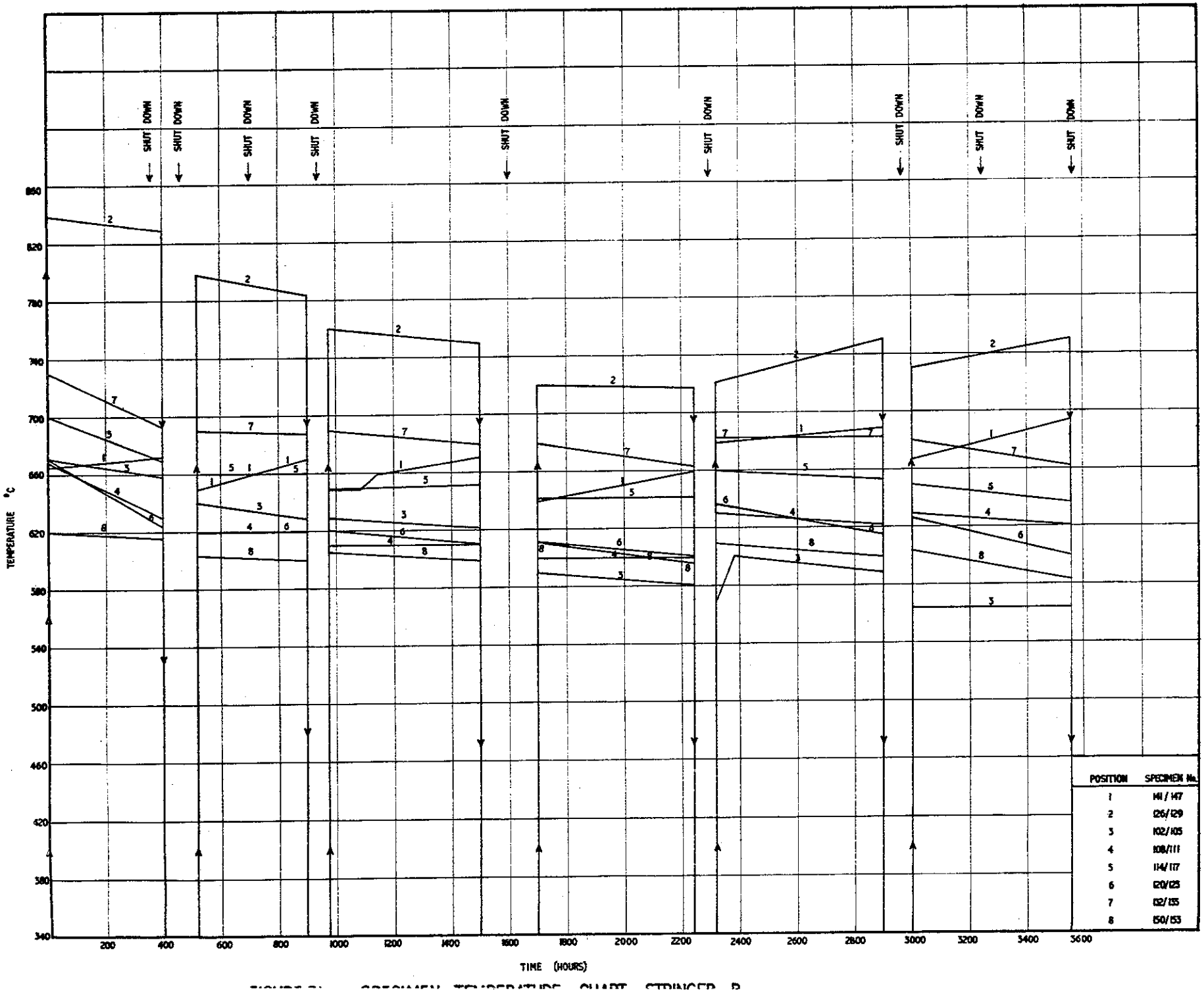
SHUT DOWN
SHUT DOWN
SHUT DOWN
SHUT DOWN
SHUT DOWN
SHUT DOWN
SHUT DOWN
SHUT DOWN
SHUT DOWN
TEMPERATURE °C
850
820
780
740
700
660
620
580
540
500
460
420
380
340
200
400
600
800
1000
1200
1400
1600
1800
2000
2200
2400
2600
2800
3000
3200
3400
3600
TIME (HOURS)
POSITION
SPECIMEN No.
1 141 / 147
2 126/129
3 102/105
4 108/111
5 114/117
6 120/123
7 132/135
8 150/153

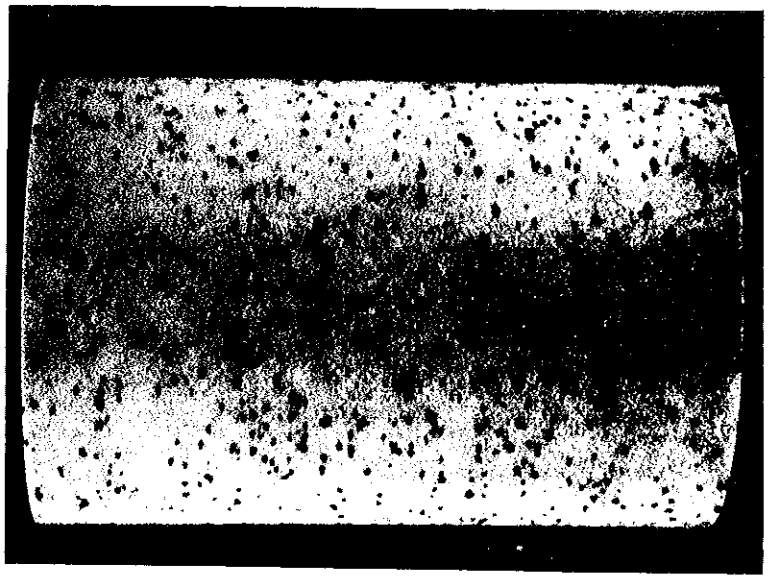

x 6

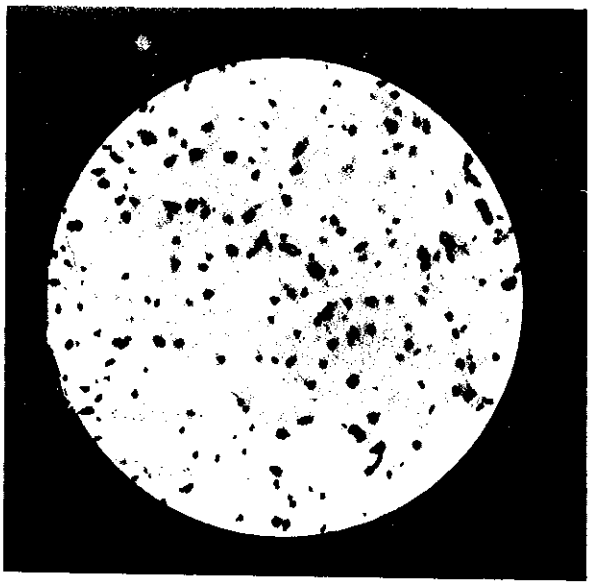

x 6

SPECIMEN 100

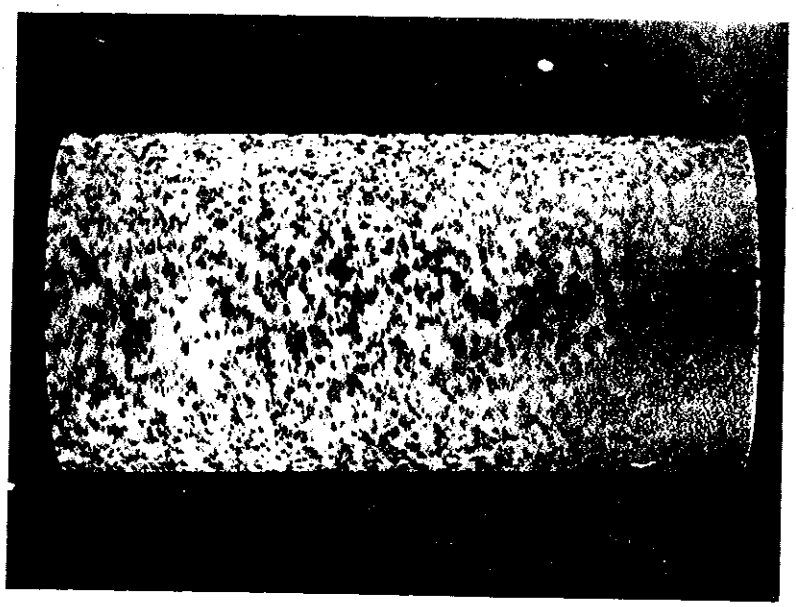

x 6

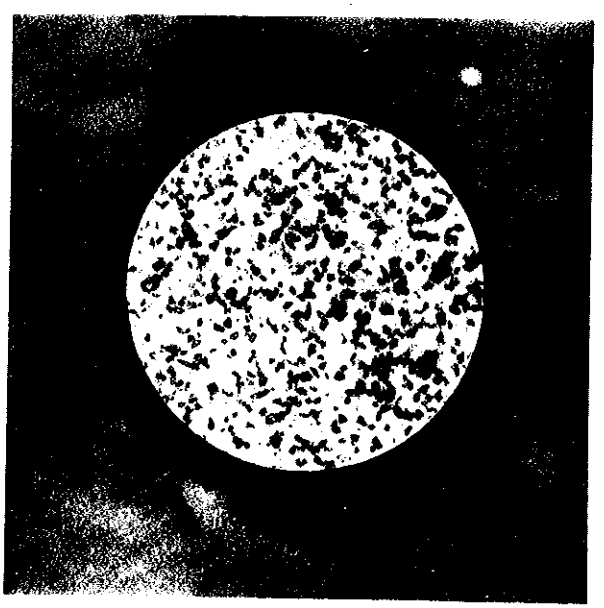

x 6

SPECIMEN 130

FIGURE 4 PHOTOGRAPHS OF SPECIMENS 100 AND 130
BEFORE IRRADIATION

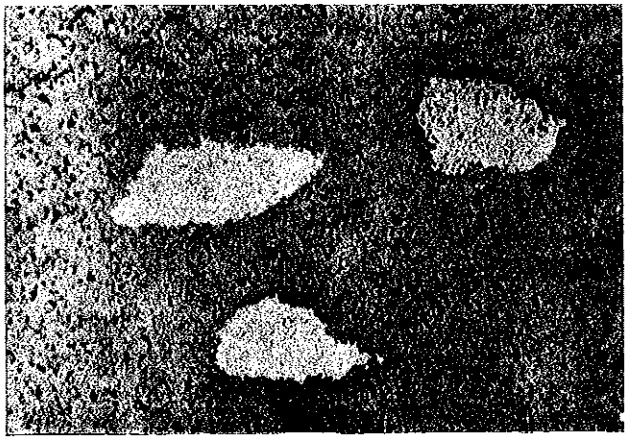

x 160

(a) Before irradiation

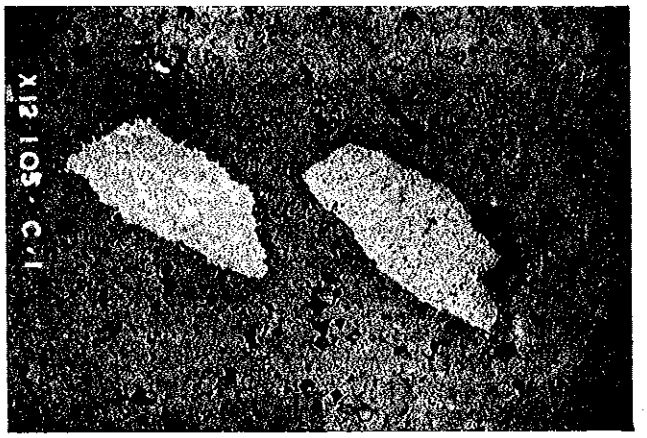

x 160

(b) After irradiation

FIGURE 5 PHOTOMICROGRAPHS OF SPECIMEN 105

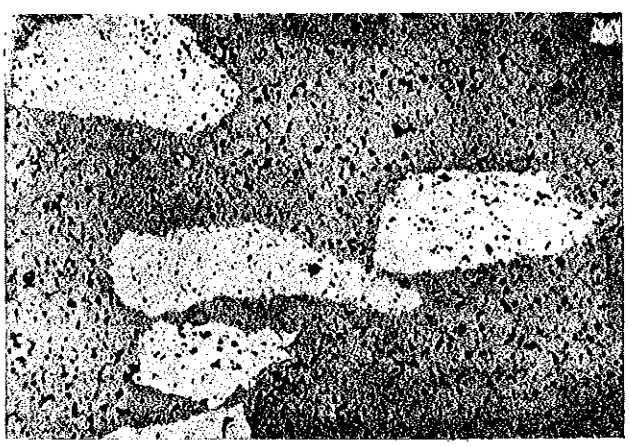

x 160

(a) Before irradiation

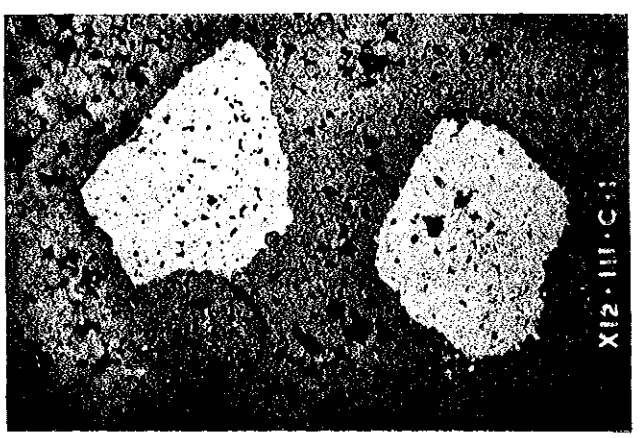

x 160

(b) After irradiation

FIGURE 6 PHOTOMICROGRAPHS OF SPECIMEN 111

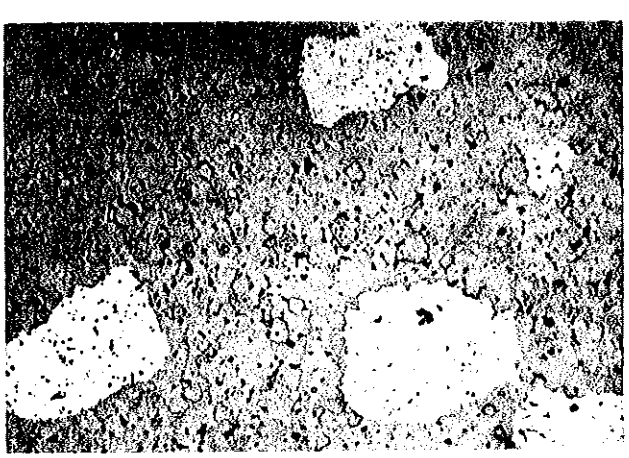

x 160

(a) Before irradiation

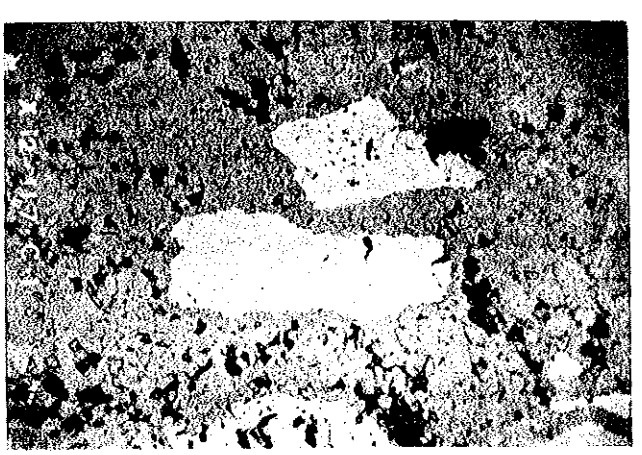

x 160

(b) After irradiation

FIGURE 7 PHOTOMICROGRAPHS OF SPECIMEN 117

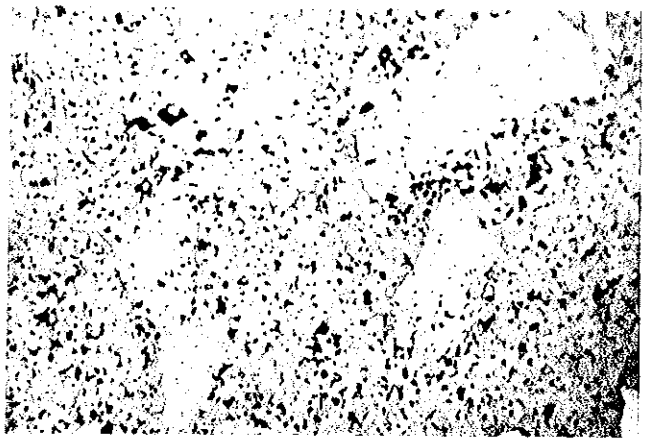

x 160

(a) Before irradiation

x 160

(b) After irradiation

FIGURE 8 PHOTOMICROGRAPHS OF SPECIMEN 123

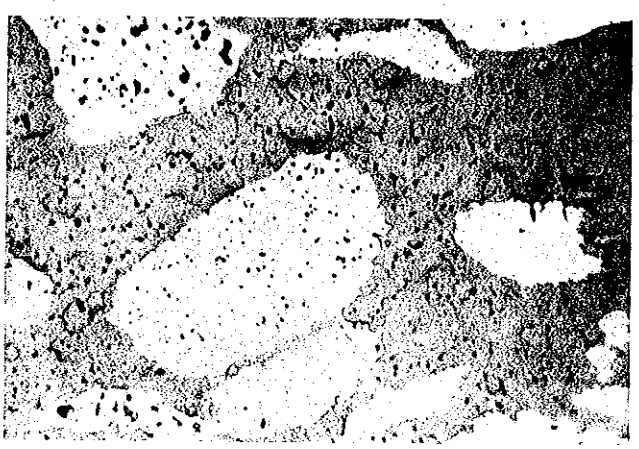

x 160

(a) Before irradiation

x 160

(b) After irradiation

FIGURE 9 PHOTOMICROGRAPHS OF SPECIMEN 129

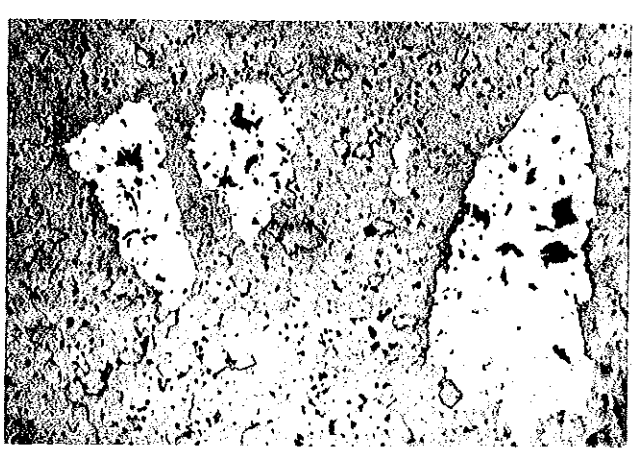

x 160

(a) Before irradiation

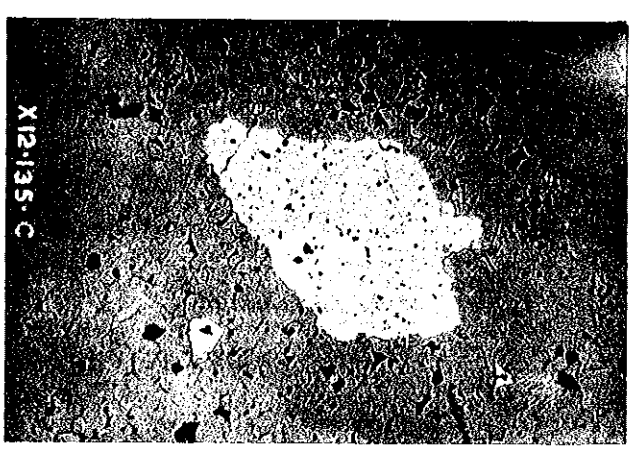

x 160

(b) After irradiation

FIGURE 10 PHOTOMICROGRAPHS OF SPECIMEN 135

x 160

(a) Before irradiation

x 160

(b) After irradiation

FIGURE 11 PHOTOMICROGRAPHS OF SPECIMEN 147

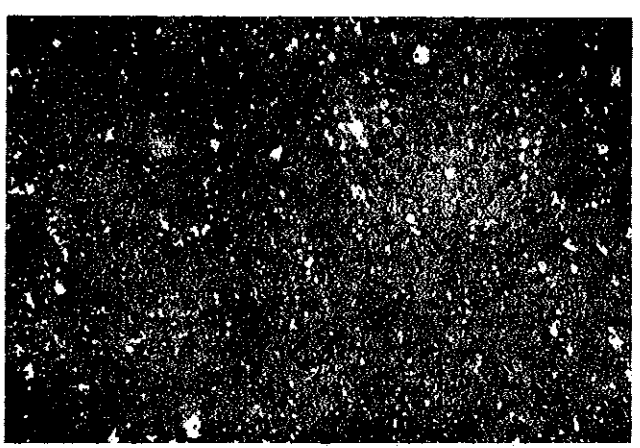

x 160

(a) Before irradiation

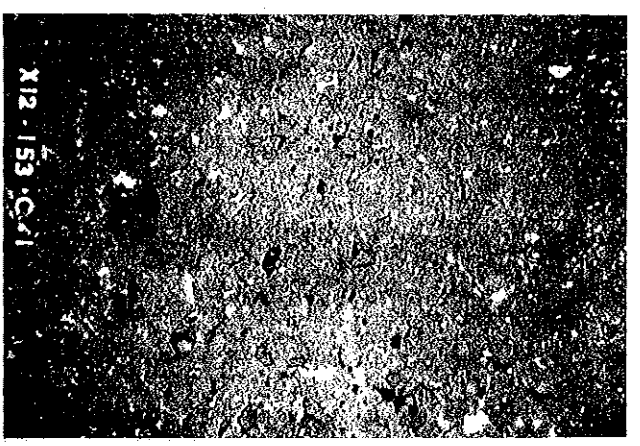

x 160

(b) After irradiation

FIGURE 12 PHOTOMICROGRAPHS OF SPECIMEN 153

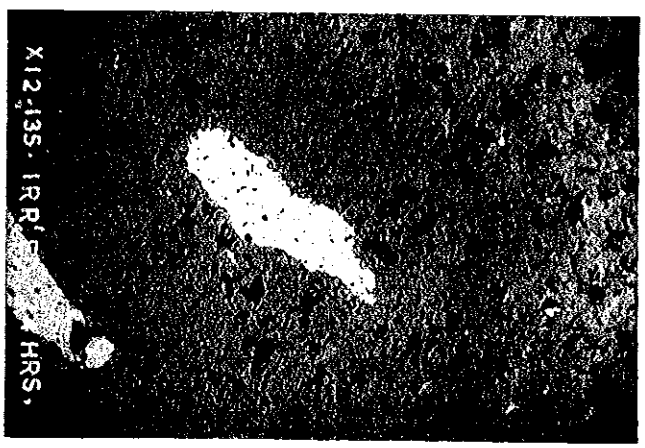

x 160

(a) After polishing for 24 hours

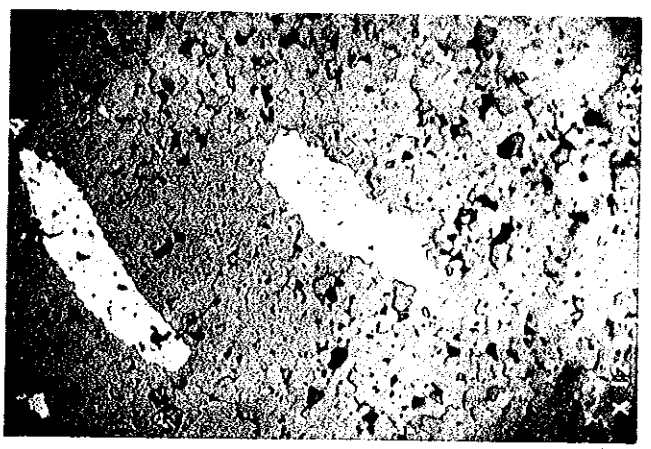

x 160

(b) After polishing for 72 hours

FIGURE 13 MICROSTRUCTURE OF IRRADIATED SPECIMEN 135

x 160

(a) Specimen 115

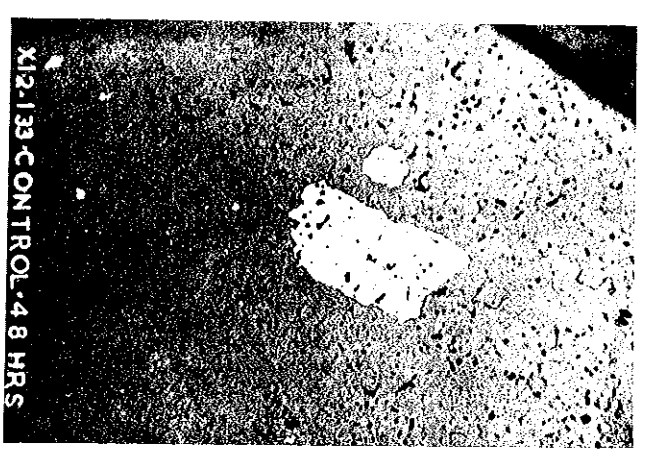

x 160

(b) Specimen 133

FIGURE 14 MICROSTRUCTURE OF HEAT–TREATED CONTROL SPECIMENS

x 1500

FIGURE 15 ELECTRON FRACTOGRAPH OF UNIRRADIATED SPECIMEN SIMILAR TO 148

x 1500

FIGURE 16 ELECTRON FRACTOGRAPH OF SPECIMEN 148 IRRADIATED TO 3×10^{19} FISSIONS cm^{-3}